

Supplementary Information

Rational Synthesis of Elusive Organic-Inorganic Hybrid Metal-oxo Clusters: Formation and Post-functionalization of Hexavanadates

*David E. Salazar Marcano,^{1‡} Givi Kalandia,^{1‡} Mhamad Aly Moussawi,¹ Kristof Van Hecke,² and
Tatjana N. Parac-Vogt^{1*}*

¹ Department of Chemistry, KU Leuven, Celestijnenlaan 200F, 3001 Leuven, Belgium

² XStruct, Department of Chemistry, Ghent University, Krijgslaan 281, S-3, 9000 Ghent, Belgium.

[‡] Authors contributed equally to this work

*E-mail: tatjana.vogt@kuleuven.be ; Tel: +32 (0)16 327612

Table of Contents

Characterization Techniques.....	3
Nuclear Magnetic Resonance (NMR) Spectroscopy	3
Fourier Transform – Infrared (FT-IR) Spectroscopy.....	3
Electrospray Ionisation Mass Spectrometry (MS).....	3
Elemental Analysis	3
Ultraviolet-Visible-Near Infrared (UV-Vis-NIR) Absorbance Spectroscopy	3
Cyclic Voltammetry (CV).....	3
Single Crystal X-ray Diffraction.....	4
Synthesis & Characterization.....	5
Synthesis of $\text{TBA}_2[\text{V}_6\text{O}_{13}\{(\text{OCH}_2)_3\text{CNHCOCH}_2\text{Cl}\}_2]$ - V ₆ -Cl.....	5
Post-functionalization of V ₆ -Cl using Na_2CO_3	6
Post-functionalization of V ₆ -Cl using TBA-OH.....	6
$\text{TBA}_2[\text{V}_6\text{O}_{13}\{(\text{OCH}_2)_3\text{CNHCOCH}_2\text{-OOC}(\text{CH}_2)_3\text{CH}_3\}_2]$ - V ₆ -Val.....	7
$\text{TBA}_2[\text{V}_6\text{O}_{13}\{(\text{OCH}_2)_3\text{CNHCOCH}_2\text{-OOCCH}_2\text{C}_6\text{H}_5\}_2]$ - V ₆ -Ph.....	7
$\text{TBA}_2[\text{V}_6\text{O}_{13}\{(\text{OCH}_2)_3\text{CNHCOCH}_2\text{-OOC}_{10}\text{H}_{15}\}_2]$ - V ₆ -Ad	8
$\text{TBA}_2[\text{V}_6\text{O}_{13}\{(\text{OCH}_2)_3\text{CNHCOCH}_2\text{-OOC}_{9}\text{H}_{15}\text{N}_2\text{OS}\}_2]$ - V ₆ -Biot	8
Solubility of Tris-R ligands	9
NMR Spectra	9
UV-Vis-NIR Absorbance.....	17
IR Spectra.....	18
ESI-MS	20
CV.....	25
References.....	25

Characterization Techniques

Nuclear Magnetic Resonance (NMR) Spectroscopy

All ^1H and ^{51}V 1D NMR spectra were acquired at 25 °C on a Bruker Avance 400 or 600 MHz spectrometer. Chemical shifts are reported relative to tetramethylsilane (TMS) for ^1H NMR spectra and VOCl_3 for ^{51}V NMR spectra.

Fourier Transform – Infrared (FT-IR) Spectroscopy

FT-IR spectra of the solid samples were acquired with a Bruker Vertex 70 FT-IR spectrometer.

Electrospray Ionisation Mass Spectrometry (MS)

ESI-MS spectra in the range 50-2000 m/z were obtained in both positive and negative ion mode on a Thermo Finnigan LCQ Advantage Mass Spectrometer with a quadrupole ion trap mass analyser or via direct injection on a Shimadzu LCMS-2020 with a DUIS-2020 ion source and a single quadrupole mass analyser.

Elemental Analysis

The C, H, and N elemental composition of samples was determined with a Flash EA-2000 CHN elemental analyser.

Ultraviolet-Visible-Near Infrared (UV-Vis-NIR) Absorbance Spectroscopy

The UV-Vis-NIR absorbance spectra of acetonitrile (ACN) solutions of V_{10} with and without the Tris-R ligands over time were acquired at room temperature with an Agilent Cary 6000i UV-Vis-NIR spectrometer. Aliquots were taken from the reaction mixture after mixing and after 0.5, 24 and 120 h of heating at 80 °C. The sample aliquots were then diluted in ACN to form a solution with a vanadium concentration of 5 mM for the absorbance measurements with clearly visible Intervalence Charge Transfer (IVCT) peaks. To observe the Ligand to Metal Charge Transfer (LMCT) peaks the solution was diluted further to obtain a vanadium concentration of 0.2 mM. All spectra were acquired in the range 200 – 1400 nm using a scan rate of 600 nm/min with the baseline corrected for with pure ACN.

Cyclic Voltammetry (CV)

Cyclic voltammograms of 0.5 mM of analyte in ACN or dimethylacetamide (DMA) were acquired at room temperature with a CH Instruments 600E potentiostat. The CV measurements were performed in an SVC-3 three-electrode cell, with a glassy carbon disc electrode (3 mm in diameter) as the working electrode, a platinum wire counter electrode and an Ag/Ag^+ reference electrode. 0.1 M tetrabutylammonium hexafluorophosphate (TBA-PF_6) was used as the electrolyte. Before all measurements, the working electrode was polished and the solution was purged with N_2 for several minutes. During measurements, the solution was kept under an N_2 atmosphere. Ferrocene was added after each measurement to determine the potential with respect to the ferrocene/ferrocenium couple (Fc/Fc^+).

Single Crystal X-ray Diffraction

The single crystals were mounted under an N₂ cryostream at 100 K and diffracted on a Rigaku Oxford Diffraction Supernova Dual Source diffractometer with an Atlas CCD detector using Cu K α ($\lambda = 1.54184 \text{ \AA}$) radiation. The images were interpreted and integrated with CrysAlisPRO¹ and the implemented face-indexed absorption correction was applied. The structures were solved using Olex2² with the ShelXT³ structure solution program using Intrinsic Phasing and refined with the ShelXL⁴ refinement package using full-matrix least squares minimization on F². Distance restraints (DFIX) were used for the amide proton. All other H atoms were placed in idealized positions and refined in riding mode. Non-hydrogen atoms were anisotropically refined and the hydrogen atoms with isotropic temperature factors were fixed at 1.2 times U_{eq} of the parent atoms (1.5 for methyl groups).

Table S1 Crystallographic parameters and refinement details for V₆-Cl and V₆-Val structures.

Compound	V ₆ -Cl	V ₆ -Val
Formula	C ₄₄ H ₉₀ Cl ₂ N ₄ O ₂₁ V ₆	C ₅₆ H ₁₁₀ Cl ₆ N ₄ O ₂₅ V
<i>FW</i> , g.mol ⁻¹	1387.8	1757.82
<i>T</i> , K	100(2)	100(2)
crystal size (mm)	0.11 × 0.06 × 0.04	0.37 × 0.08 × 0.05
crystal system	Triclinic	Monoclinic
space group	<i>P</i> -1	<i>P</i> 2 ₁ / <i>c</i>
<i>a</i> , Å	10.7293(6)	10.63100(10)
<i>b</i> , Å	11.8938(8)	19.7400(2)
<i>c</i> , Å	12.7361(8)	18.5098(2)
α , °	112.102(6)	90
β , °	97.669(5)	90.0190(10)
γ , °	93.798(5)	90
<i>V</i> , Å ³	1480.33(18)	3884.39(7)
<i>Z</i>	1	2
ρ_{calc} , g.cm ⁻³	1.557	1.503
μ (Cu K α), mm ⁻¹	9.091	8.333
λ (Cu K α), Å	1.54184	1.54184
2 θ range	7.604° ≤ 2 θ ≤ 148.136°	6.546° ≤ 2 θ ≤ 147.662°
data collected	27888	19898
unique data	5919	7301
unique data I ≥ 2 σ (I)	4169	6027
no. Parameters	356	447
restraints	1	1
<i>R</i> ₁	0.0547	0.0418
<i>wR</i> ₂	0.1567	0.1057
GOF	1.025	1.095

Synthesis & Characterization

All reagents and solvents were used as obtained from commercial sources without further purification. The synthesis precursors for $\text{TBA}_2[\text{V}_6\text{O}_{13}\{(\text{OCH}_2)_3\text{CNHCOCH}_2\text{Cl}\}_2]$ ($\text{V}_6\text{-Cl}$; $\text{TBA} = (\text{C}_4\text{H}_9)_4\text{N}^+$) – tetrabutylammonium decavanadate ($\text{TBA}_3[\text{H}_3\text{V}_{10}\text{O}_{28}]$; V_{10}) and chloro-N-(1,3-dihydroxy-2-(hydroxymethyl)prop-2-yl)acetamide ($\text{ClCH}_2\text{CONHC}(\text{CH}_2\text{OH})_3$; Tris-Cl) – were synthesized and characterized based on previously reported procedures.^{5,6} Post-functionalization of $\text{V}_6\text{-Cl}$ was attempted using either Na_2CO_3 or tetrabutylammonium hydroxide (TBA-OH) as the base according to previously reported procedures.⁶ Both methods were successful for $\text{V}_6\text{-Val}$, $\text{V}_6\text{-Ph}$ and $\text{V}_6\text{-Ad}$. Synthesis of $\text{V}_6\text{-Biot}$ was only attempted using TBA-OH . The yields and characterization data for all the compounds are reported according to the results from the post-functionalization of $\text{V}_6\text{-Cl}$ using Na_2CO_3 since this procedure gave the highest yields and purity for all compounds except for $\text{V}_6\text{-Biot}$, which could be obtained in relatively high yields using TBA-OH .

Synthesis of $\text{TBA}_2[\text{V}_6\text{O}_{13}\{(\text{OCH}_2)_3\text{CNHCOCH}_2\text{Cl}\}_2]$ - $\text{V}_6\text{-Cl}$

1.6878 g of V_{10} (1.0 mmol, 1 eq) and 0.6918 g of Tris-Cl (3.5 mmol, 3.5 eq), which had been previously vacuum-dried, were placed under argon atmosphere and dissolved in 35 mL of dry DMA to form a dark orange solution. The reaction mixture was then stirred at 80 °C while covered in aluminium foil and the solution eventually turned green. After 5 days, the reaction mixture was allowed to cool down to room temperature and DMA was removed via rotary evaporation. Evaporation resulted in a green residue to which a small amount of ACN was added. Most of the residue dissolved immediately giving a green solution, but a small amount of red/orange solid was left undissolved, which proved to be the desired $\text{V}_6\text{-Cl}$. The mixture was then separated via centrifugation. 35 wt% H_2O_2 (~0.5 mL) was added to the green supernatant until it turned red/orange and a small amount of precipitate was observed (due to the protonated form of the product). The mixture was once again centrifuged and the supernatant was added to an excess amount of Et_2O to form a dark red solid, which was separated via centrifugation. A small amount of water was added to the solid and the mixture was sonicated until the solid was broken up into a dispersion of small particles. The mixture was then centrifuged and the solid was redissolved in a minimal amount of MeOH, to then be precipitated out again by adding it to excess Et_2O . The re-precipitation with excess Et_2O was then repeated after re-dissolving the precipitate in ACN. The solid obtained through the purification procedure and the original red/orange solid observed after re-dissolving the reaction mixture were combined as they were both determined to be the pure product. To obtain crystals, the pure product was dissolved in a minimum amount of ACN and placed in a sealed container with Et_2O for slow vapor diffusion. Yield: 0.8460 g, 61%.

Elemental analysis (%) for $\text{C}_{44}\text{H}_{90}\text{C}_{12}\text{N}_4\text{O}_{21}\text{V}_6$ (1387.75 g mol^{-1}): calcd. = C 38.08, H 6.54, N 4.04; found = C 37.93, H 6.45, N 3.88.

ESI-MS (negative mode, ACN, $\text{M} = [\text{V}_6\text{O}_{13}\{(\text{OCH}_2)_3\text{CNHCOCH}_2\text{Cl}\}_2]^{2-}$): $m/z = 1145.8$ ($[\text{M}+\text{TBA}]^-$, calcd. $m/z = 1145.3$).

ESI-MS (positive mode, ACN, $M = [V_6O_{13}\{(OCH_2)_3CNHCOCH_2Cl\}_2]^{2-}$): $m/z = 1630.1$ ($[M+3TBA]^+$, calcd. $m/z = 1630.2$).

FT-IR: $\tilde{\nu}$ (cm^{-1}) = 3280 (v N-H, w), 3234 (v N-H, w), 3052 (w), 2960 (v C-H, w), 2936 (v C-H, w), 2865 (v C-H, w), 1692 (v C=O, m), 1677 (m), 1622 (w), 1539 (m), 1482 (δ C-H, m), 1464 (δ C-H, m), 1409 (w), 1379 (δ C-H, m), 1325 (w), 1220 (w), 1183 (w), 1150 (w), 1114 (v C-O, m), 1063 (v C-O, s), 999 (w), 961 (v V=O, s), 940 (v V=O, vs), 931 (v V=O, vs), 888 (w), 799 (v V-O-V, s), 789 (v V-O-V, s), 716 (v V-O-V, vs), 628 (m), 578 (s), 511 (s), 472 (s), 457 (s), 411 (vs).

1H NMR (400 MHz, DMSO- d_6): δ (ppm) = 7.83 (s, 2H, NH), 5.11 (s, 12H, CH_2O), 4.02 (s, 4H, CH_2Cl), 3.13 (m, 16H, H_{TBA}), 1.57 (m, 16H, H_{TBA}), 1.30 (m, 16H, H_{TBA}), 0.94 (t, 24H, H_{TBA}).

^{51}V NMR (400 MHz, DMSO- d_6): δ (ppm) = -494.47 (s).

Post-functionalization of V₆-Cl using Na₂CO₃

0.0555 g of V₆-Cl (0.04 mmol, 1 eq), 0.0148 g of TBA-I (0.04 mmol, 1 eq) and 5 eq of carboxylic acid, which had been previously vacuum-dried, were dissolved in 3 mL of dry DMA. After everything dissolved to form an orange solution, 0.0169 g of Na₂CO₃ (0.16 mmol, 4 eq) was added. The reaction mixture was stirred for 2-5 h at 80 °C under an argon atmosphere. After the reaction mixture cooled down, it was centrifuged to remove any residual solid. DMA was then removed from the supernatant by rotary evaporation and the obtained residue was redissolved in 5 mL of ACN. If a green solution was obtained, due to the presence of mixed valence species, 35 wt% H₂O₂ (~0.01 mL) was added to the solution to fully oxidize the species, resulting in an orange solution. The ACN solution was then added dropwise to an excess of Et₂O and the precipitate was recovered by centrifugation. The solid was then re-dissolved in ACN and precipitated out of solution with excess Et₂O. This process was repeated until the pure product was obtained. Impurities that could not be removed in this way for some of the samples were removed by re-dissolving the solid in MeOH and precipitating it out with Et₂O and/or by washing the product with a minimum amount of water, before a final re-precipitation from ACN with Et₂O.

Post-functionalization of V₆-Cl using TBA-OH

104 μ L of TBA-OH (0.16 mmol, 4 eq) were added to 0.5 mL of dry DMA followed by 5 eq of carboxylic acid and the mixture was stirred at room temperature for at least 5 min. Separately, 0.0555 g of V₆-Cl (0.04 mmol, 1 eq) and 0.0148 g of TBA-I (0.04 mmol, 1 eq) were dissolved in 2.5 mL of dry DMA. Once dissolved, the POM solution was transferred to the solution with the carboxylic acid. Then, the reaction mixture was stirred at 80 °C for 2 h. The pure product was obtained following the same purification steps described for post-functionalization of V₆-Cl using Na₂CO₃.

TBA₂[V₆O₁₃{(OCH₂)₃CNHCOCH₂-OOC(CH₂)₃CH₃}₂] - V₆-Val

Yield: 0.0335 g, 55%.

Elemental analysis (%) for C₅₄H₁₀₈N₄O₂₅V₆ (1519.10 gmol⁻¹): calcd. = C 42.69, H 7.17, N 3.69; found = C 42.23, H 7.14, N 3.44.ESI-MS (negative mode, ACN, M = [V₆O₁₃{(OCH₂)₃CNHCOCH₂-OOC(CH₂)₃CH₃}₂]²⁻): *m/z* = 517.5 ([M]²⁻, calcd. *m/z* = 517.1), 1276.2 ([M+TBA]⁻, calcd. *m/z* = 1276.6).ESI-MS (positive mode, ACN, M = [V₆O₁₃{(OCH₂)₃CNHCOCH₂-OOC(CH₂)₃CH₃}₂]²⁻): *m/z* = 1760.2 ([M+TBA]⁺, calcd. *m/z* = 1761.6).FT-IR: $\tilde{\nu}$ (cm⁻¹) = 3282 (v N-H, w), 3249 (v N-H, w), 3081 (w), 2960 (v C-H, m), 2934 (v C-H, w), 2873 (v C-H, w), 1742 (v C=O, m), 1708 (v C=O, m), 1560 (m), 1465 (δ C-H, m), 1422 (w), 1379 (δ C-H, m), 1328 (w), 1308 (w), 1270 (w), 1252 (w), 1230 (m), 1182 (m), 1165 (m), 1107 (v C-O, m), 1092 (m), 1067 (v C-O, s), 1035 (v C-O, m), 994 (w), 948 (v V=O, vs), 934 (v V=O, vs), 887 (w), 808 (v V-O-V, s), 795 (v V-O-V, s), 719 (v V-O-V, vs), 580 (s), 513 (s), 484 (s), 459 (s), 414 (vs).¹H NMR (400 MHz, DMSO-d₆): δ (ppm) = 7.59 (s, 2H, NH), 5.09 (s, 12H, CH₂O), 4.42 (s, 4H, CH₂OOC), 3.17 (m, 16H, H_{TBA}), 2.33 (t, ³J = 7.4 Hz, 4H, CH₂OOC), 1.57 (m, 16H, H_{TBA}), 1.51 (m, 4H, CH₂), 1.30 (m, 20H, H_{TBA} and CH₂), 0.94 (t, 24H, H_{TBA}), 0.86 (t, ³J = 7.4 Hz, 6H, CH₃).⁵¹V NMR (400 MHz, DMSO-d₆): δ (ppm) = -494.62 (s).**TBA₂[V₆O₁₃{(OCH₂)₃CNHCOCH₂-OOCCH₂C₆H₅}₂] - V₆-Ph**

Yield: 0.0247 g, 41%.

Elemental analysis (%) for C₆₀H₁₀₄N₄O₂₅V₆ (1587.13 gmol⁻¹): calcd. = C 45.41, H 6.60, N 3.53; found = C 44.72, H 6.41, N 3.35.ESI-MS (negative mode, ACN, M = [V₆O₁₃{(OCH₂)₃CNHCOCH₂-OOCCH₂C₆H₅}₂]²⁻): *m/z* = 551.2 ([M]²⁻, calcd. *m/z* = 551.1), 1344.1 ([M+TBA]⁻, calcd. *m/z* = 1344.7).ESI-MS (positive mode, ACN, M = [V₆O₁₃{(OCH₂)₃CNHCOCH₂-OOCCH₂C₆H₅}₂]²⁻): *m/z* = 1828.1 ([M+TBA]⁺, calcd. *m/z* = 1829.6).FT-IR: $\tilde{\nu}$ (cm⁻¹) = 3288 (v N-H, w), 3074 (w), 2961 (v C-H, w), 2935 (v C-H, w), 2874 (v C-H, w), 1739 (v C=O, m), 1709 (v C=O, m), 1694 (v C=O, m), 1645 (w), 1603(w), 1557 (m), 1497 (w), 1470 (δ C-H, m), 1420 (w), 1380 (δ C-H, w), 1346 (w), 1308 (w), 1276 (w), 1225 (m), 1190 (w), 1141 (m), 1115 (v C-O, w), 1069 (v C-O, s), 1040 (m), 945 (v V=O, s), 932 (v V=O, s), 881 (w), 809 (v V-O-V, s), 797 (v V-O-V, s), 719 (v V-O-V, vs), 581 (s), 561(m), 513 (s), 480 (s), 459 (s), 413 (vs).¹H NMR (400 MHz, DMSO-d₆): δ (ppm) = 7.59 (s, 2H, NH), 7.29 (m, 10H, C₆H₅), 5.09 (s, 12H, CH₂O), 4.46 (s, 4H, CH₂OOC), 3.73 (s, 4H, OOCCH₂), 3.17 (m, 16H, H_{TBA}), 1.57 (m, 16H, H_{TBA}), 0.94 (t, 24H, H_{TBA}).

^{51}V NMR (400 MHz, DMSO- d_6): δ (ppm) = -494.96 (s).

TBA₂[V₆O₁₃{(OCH₂)₃CNHCOCH₂-OOC C₁₀H₁₅}₂] - V₆-Ad

Yield: 0.0306 g, 50%.

Elemental analysis (%) for C₆₆H₁₂₀N₄O₂₅V₆ (1675.32 gmol⁻¹): calcd. = C 47.32, H 7.22, N 3.34; found = C 46.52, H 6.71, N 3.32.

ESI-MS (negative mode, ACN, M = [V₆O₁₃{(OCH₂)₃CNHCOCH₂-OOC C₁₀H₁₅}₂]²⁻): m/z = 595.5 ([M]²⁻, calcd. m/z = 595.2), 1432.1 ([M+TBA]⁻, calcd. m/z = 1432.9).

ESI-MS (positive mode, ACN, M = [V₆O₁₃{(OCH₂)₃CNHCOCH₂-OOC C₁₀H₁₅}₂]²⁻): m/z = 1916.3 ([M+TBA]⁺, calcd. m/z = 1917.8).

FT-IR: $\tilde{\nu}$ (cm⁻¹) = 3280 (v N-H, w), 3247 (v N-H, w), 3076 (w), 2959 (v C-H, m), 2905 (v C-H, m), 2874 (v C-H, m), 2852 (v C-H, w), 1728 (v C=O, m), 1704 (v C=O, m), 1555 (m), 1453 (δ C-H, m), 1421 (w), 1380 (δ C-H, w), 1345 (w), 1325 (w), 1310 (w), 1276 (w), 1269 (w), 1226 (s), 1183 (m), 1103 (v C-O, w), 1086 (v C-O, s), 1065 (m), 952 (v V=O, s), 936 (v V=O, s), 880 (w), 808 (v V-O-V, s), 796 (v V-O-V, s), 768 (w), 719 (v V-O-V, vs), 670 (m), 580 (s), 561 (m), 512 (w), 481 (s), 458 (s), 413 (s).

^1H NMR (400 MHz, DMSO- d_6): δ (ppm) = 7.56 (s, 2H, NH), 5.08 (s, 12H, CH₂O), 4.42 (s, 4H, CH₂OOC), 3.17 (m, 16H, H_{TBA}), 1.96 (s, 6H, CH), 1.83 (s, 12H, CH₂), 1.66 (s, 12H, CH₂), 1.57 (m, 16H, H_{TBA}), 1.31 (m, 16H), 0.94 (t, 24H, H_{TBA}).

^{51}V NMR (400 MHz, DMSO- d_6): δ (ppm) = -493.81 (s).

TBA₂[V₆O₁₃{(OCH₂)₃CNHCOCH₂-OOC C₉H₁₅N₂OS}₂] - V₆-Biot

Yield: 0.0470 g, 65%.

Elemental analysis (%) for C₆₄H₁₂₀N₈O₂₇S₂V₆ (1803.46 gmol⁻¹): calcd. = C 42.62, H 6.71, N 6.21; found = C 43.07, H 6.06, N 6.19.

ESI-MS (negative mode, ACN, M = [V₆O₁₃{(OCH₂)₃CNHCOCH₂-OOC C₉H₁₅N₂OS}₂]²⁻): m/z = 659.6 ([M]²⁻, calcd. m/z = 659.3), 1319.2 ([M+H]⁻, calcd. m/z = 1319.5), 1560.3 ([M+TBA]⁻, calcd. m/z = 1561.0).

FT-IR: $\tilde{\nu}$ (cm⁻¹) = 3284 (v N-H, w), 3068 (w), 2960 (v C-H, w), 2933 (v C-H, w), 2872 (v C-H, w), 1737 (v C=O, m), 1683 (v C=O, s), 1544 (w), 1460 (δ C-H, m), 1427 (w), 1380 (δ C-H, w), 1329 (w), 1310 (w), 1260 (w), 1234 (w), 1158 (w), 1118 (w), 1070 (v C-O, m), 948 (v V=O, vs), 882 (w), 809 (v V-O-V, s), 796 (v V-O-V, s), 758 (m), 715 (v V-O-V, vs), 577 (s), 512 (m), 462 (m), 414 (vs).

^1H NMR (400 MHz, DMSO- d_6): δ (ppm) = 7.61 (s, 2H, NH), 6.41 (s, 2H, CNHCON), 6.33 (s, 2H, CNHCON), 5.09 (s, 12H, CH₂OOC), 4.43 (s, 4H, CH₂OOC), 4.30 (m, 2H, CHN), 4.13 (m, 2H,

CHN), 3.17 (m, 16H, H_{TBA}), 3.09 (m, 2H, CHS), 2.83 (dd, ²J = 5.2 Hz, ³J = 12.5 Hz, 2H, SCH₂), 2.57 (d, ³J = 12.5 Hz, 2H, SCH₂), 2.34 (t, ³J = 7.3 Hz, 4H, OOCCH₂), 1.57 (m, 24H, 16H_{TBA} & 8H CH₂), 1.32 (m, 20H, 16H_{TBA} & 4H CH₂), 0.94 (t, 24H, H_{TBA}).

⁵¹V NMR (400 MHz, DMSO-d₆): δ (ppm) = -493.69 (s).

Solubility of Tris-R ligands

Table S2 Approximate solubility of Tris-R ligands.

Solvent	Ligand	Solubility / mgmL ⁻¹
ACN	Tris-CH ₃	15
	Tris-NH ₂	< 1
	Tris-Cl	29
DMA	Tris-Cl	600

NMR Spectra

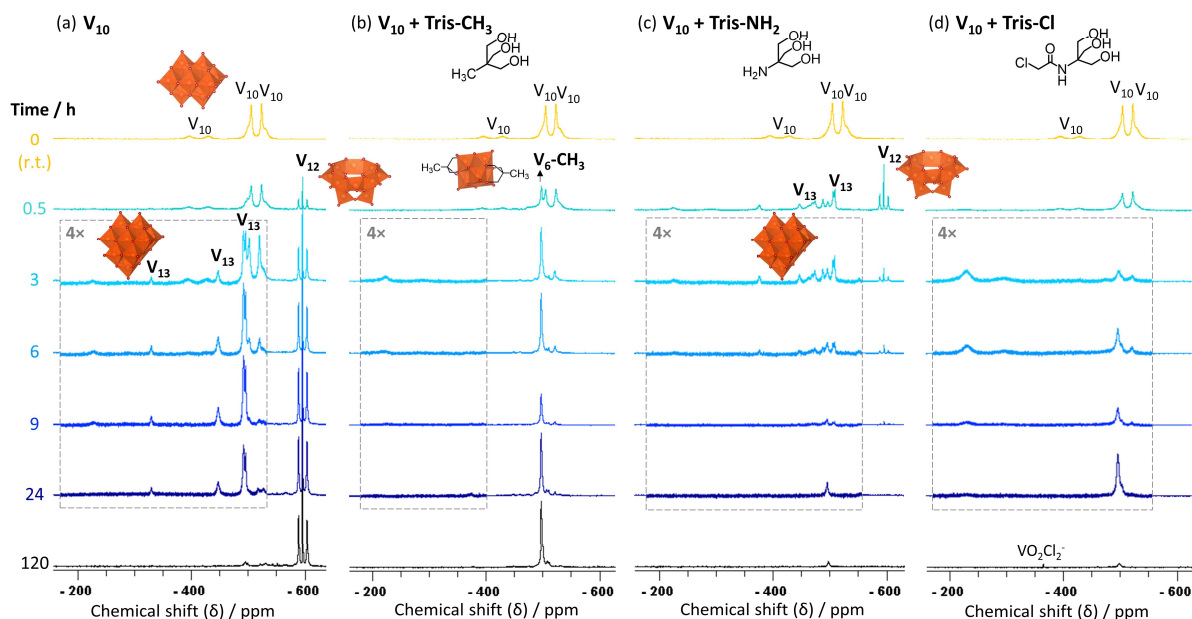


Figure S1 ⁵¹V NMR spectra of 10 mM V₁₀ (a) alone as well as with (b) Tris-CH₃, (c) Tris-NH₂, or (d) Tris-Cl in ACN-d₃ after mixing at room temperature (r.t.) and after 0.5, 3, 6, 9, 24 and 120 h at 80 °C. The relative intensity of some regions of the spectra (between -150 and -550 ppm) acquired after 3-24 h was increased by a factor of 4 to show relatively weak peaks.

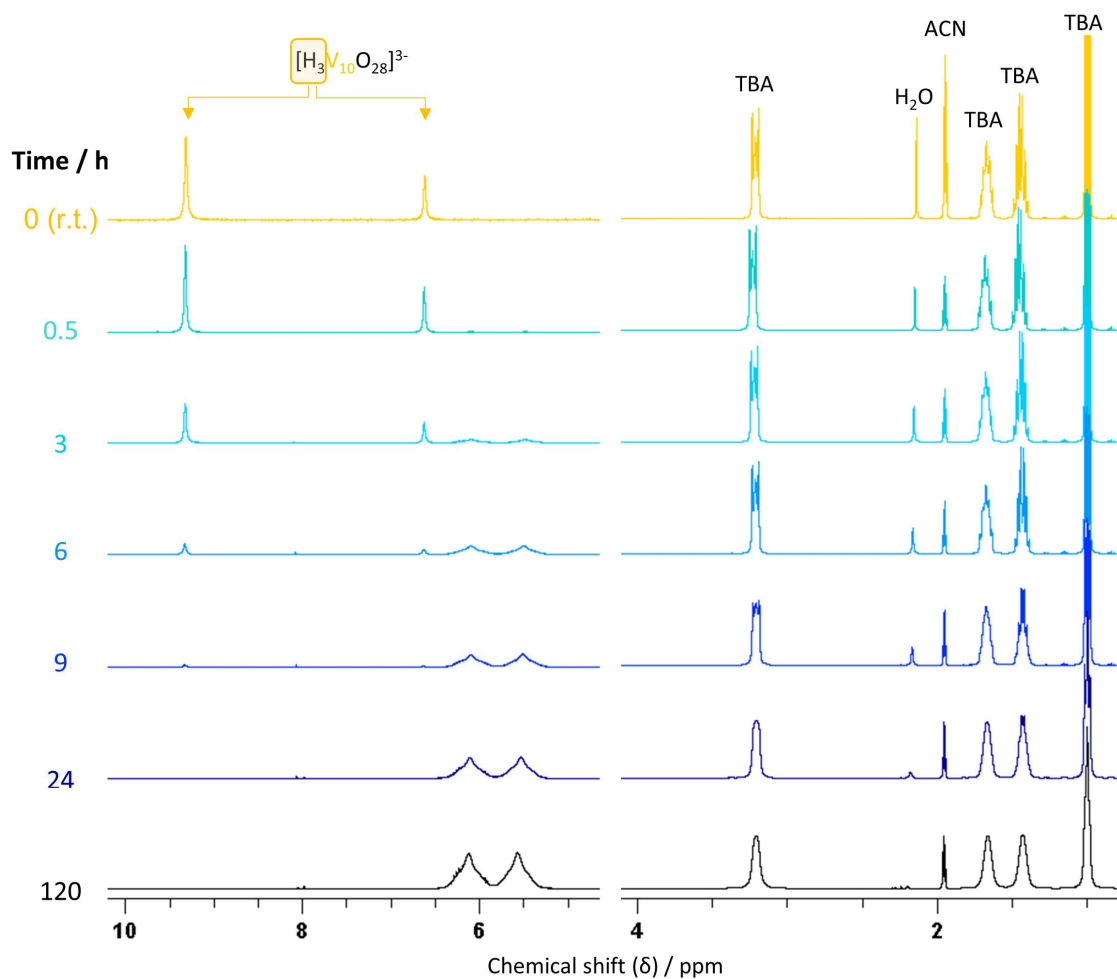


Figure S2 ^1H NMR spectra of 10 mM V_{10} alone in ACN-d_3 at room temperature (r.t.) and after 0.5, 3, 6, 9, 24 and 120 h of heating at 80 °C. The intensity of the peaks in the range 4-10 ppm is significantly weaker than that of the peaks in the rest of the spectrum.

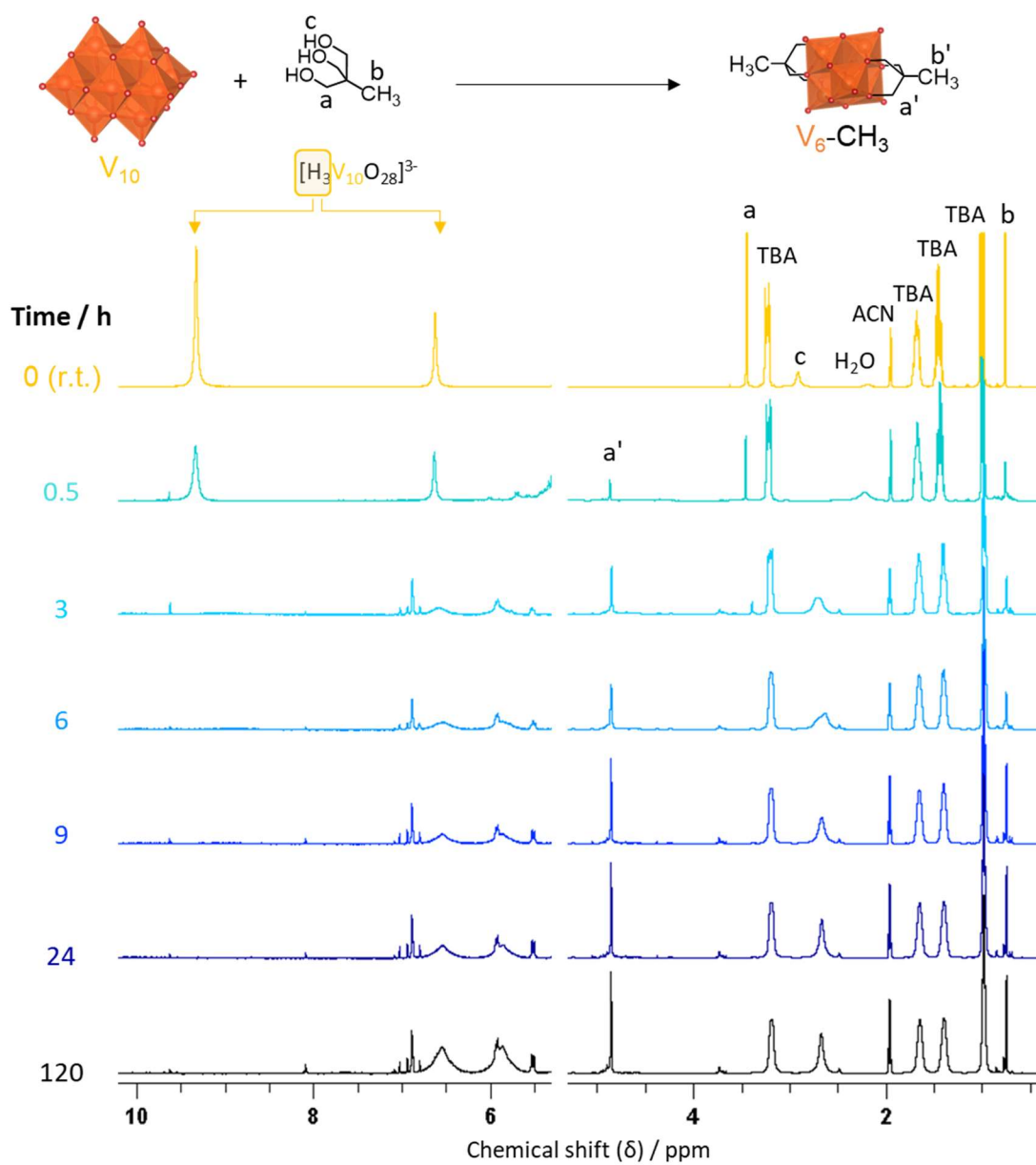


Figure S3 ^1H NMR spectra of V_{10} (10 mM) and Tris-CH_3 (1:2 ratio) at room temperature (r.t.) and after 0.5, 3, 6, 9, 24 and 120 h of heating at 80 °C. The intensity of the peaks in the range 5-10 ppm is significantly weaker than that of the peaks in the rest of the spectrum.

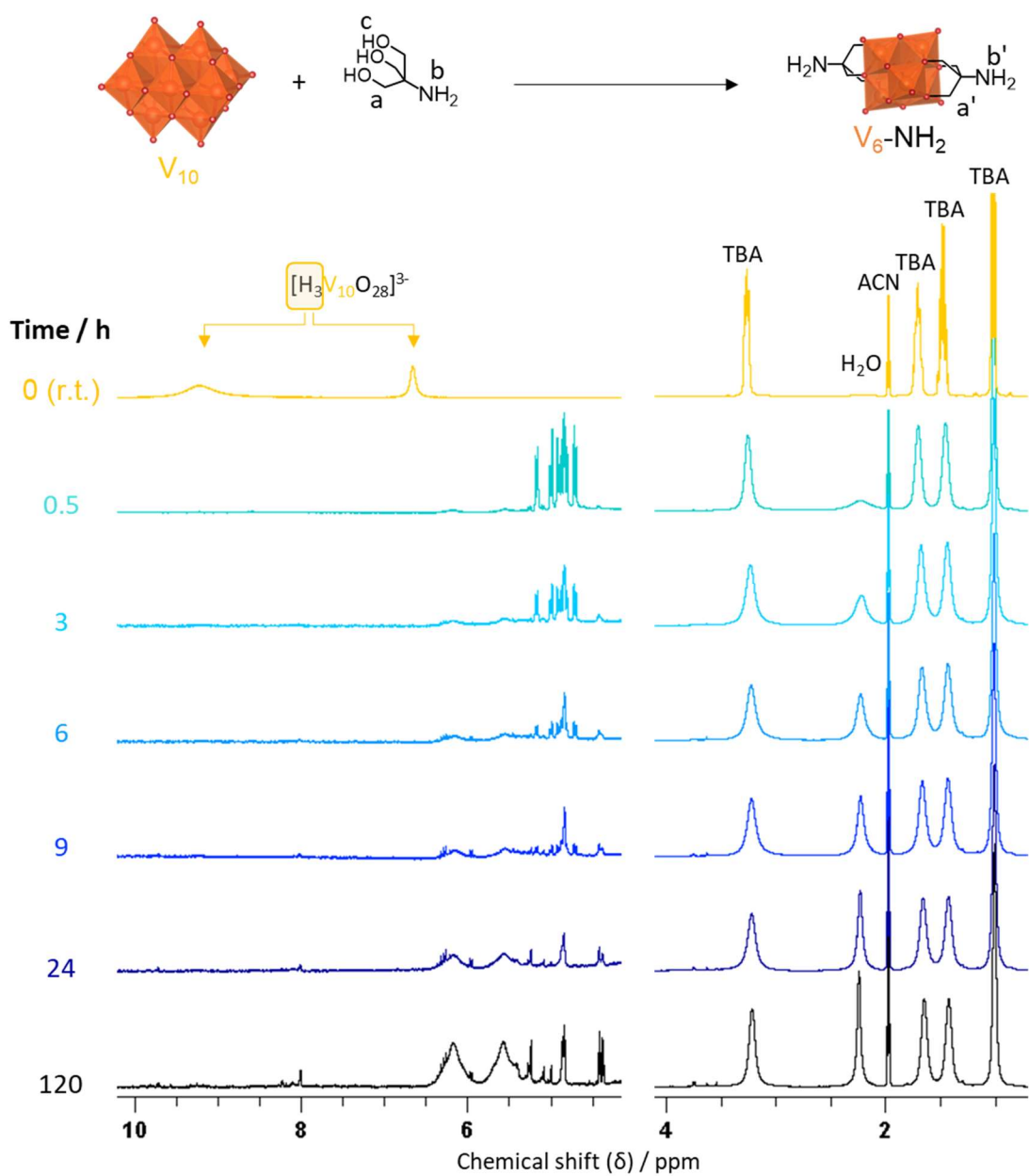


Figure S4 ^1H NMR spectra of V_{10} (10 mM) and Tris- NH_2 (1:2 ratio) at room temperature (r.t.) and after 0.5, 3, 6, 9, 24 and 120 h of heating at 80°C . The intensity of the peaks in the range 5-10 ppm is significantly weaker than that of the peaks in the rest of the spectrum.

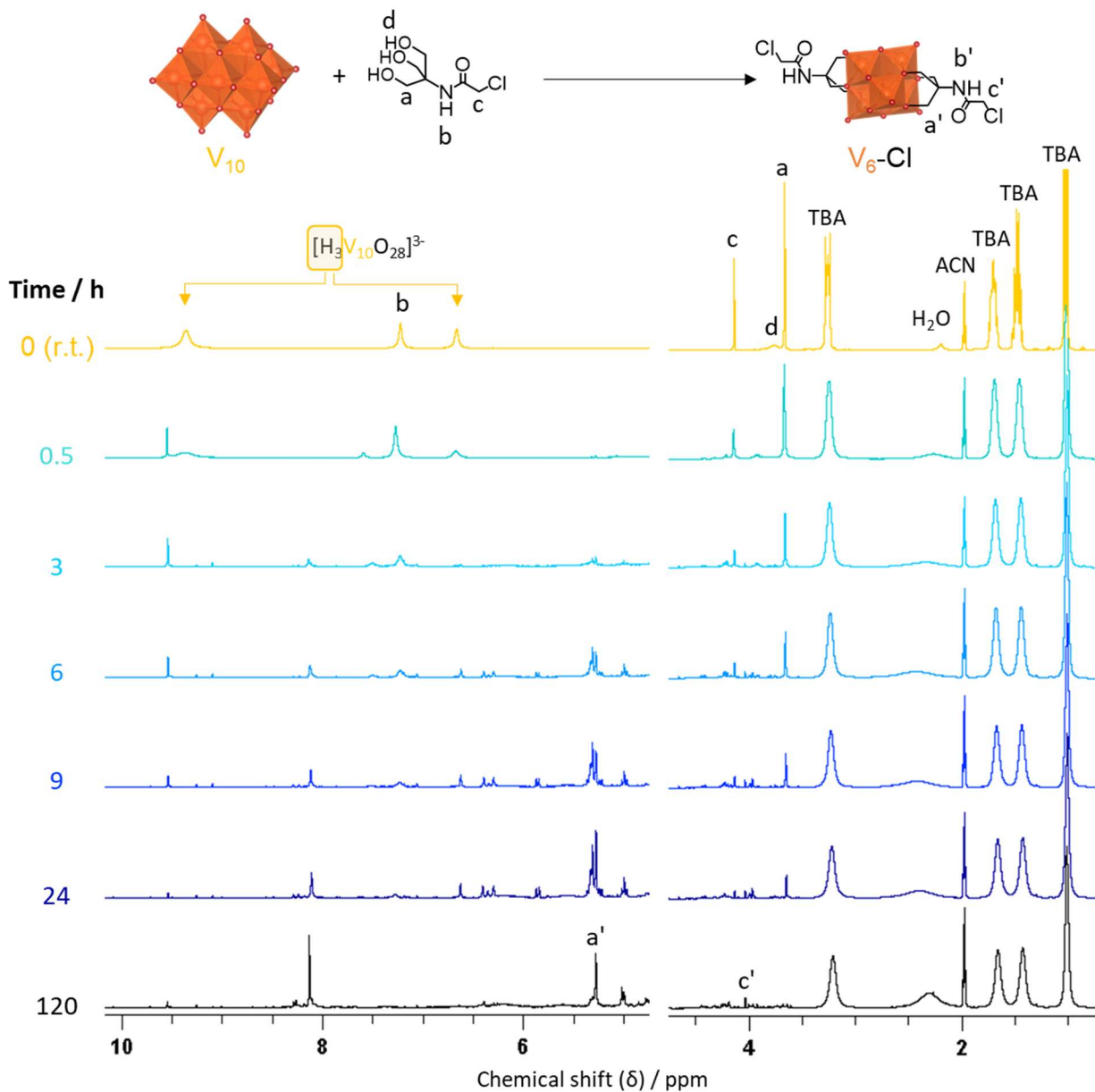


Figure S5 ^1H NMR spectra of V_{10} (10 mM) and Tris-Cl (1:2 ratio) at room temperature (r.t.) and after 0.5, 3, 6, 9, 24 and 120 h of heating at 80°C . The intensity of the peaks in the range 5-10 ppm is significantly weaker than that of the peaks in the rest of the spectrum.

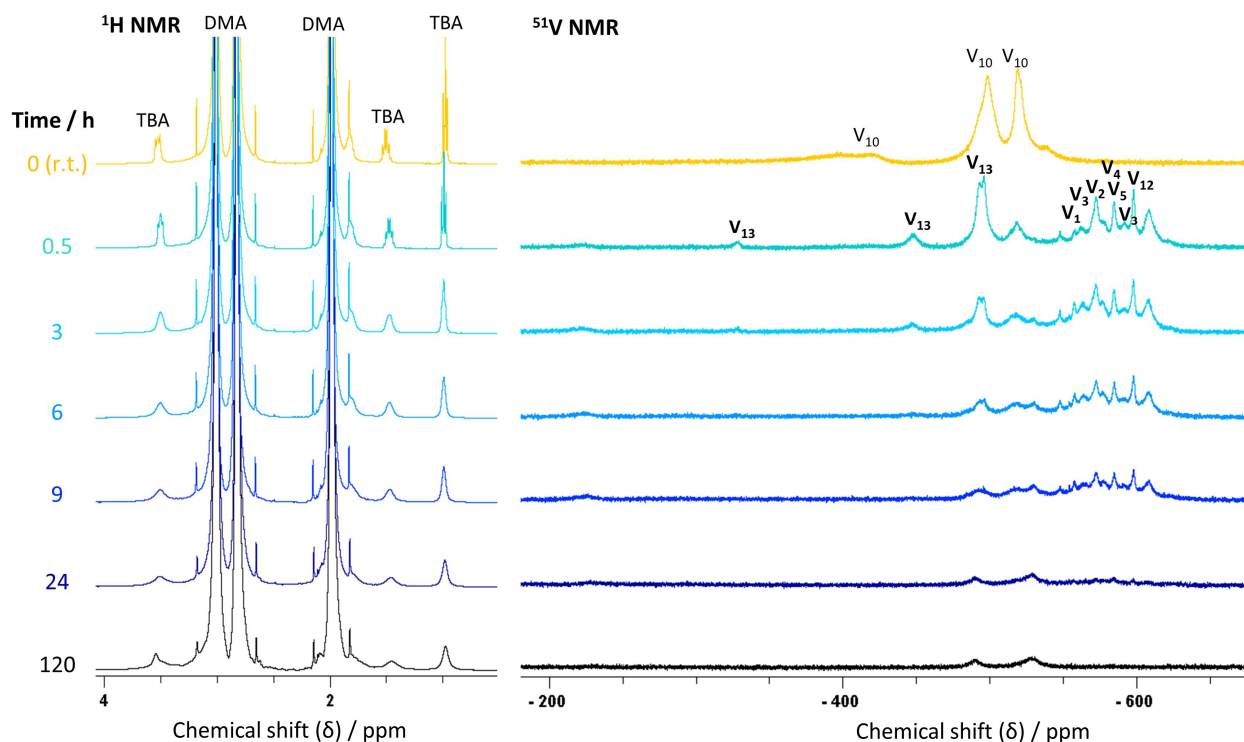


Figure S6 ^1H and ^{51}V NMR spectra of 10 mM V_{10} alone in DMA (with 10% of acetone- d_6 for locking) at room temperature (r.t.) and after 0.5, 3, 6, 9, 24 and 120 h of heating at 80 °C. Several overlapping peaks (between -500 and -650 ppm) that could correspond to different vanadate species of varying nuclearity were observed to appear after heating for 0.5 h: $[\text{VO}_2(\text{H}_2\text{O})]^+$ or $[\text{H}_2\text{VO}_4]^-$ (V_1), $[\text{H}_n\text{V}_2\text{O}_7]^{(4-n)-}$ (V_2), $[\text{V}_3\text{O}_{10}]^{5-}$ (V_3), $[\text{V}_4\text{O}_{13}]^{6-}$ (V_4), $[\text{V}_5\text{O}_{15}]^{5-}$ (V_5) and $[\text{V}_{12}\text{O}_{32}]^{4-}$ (V_{12}).⁷

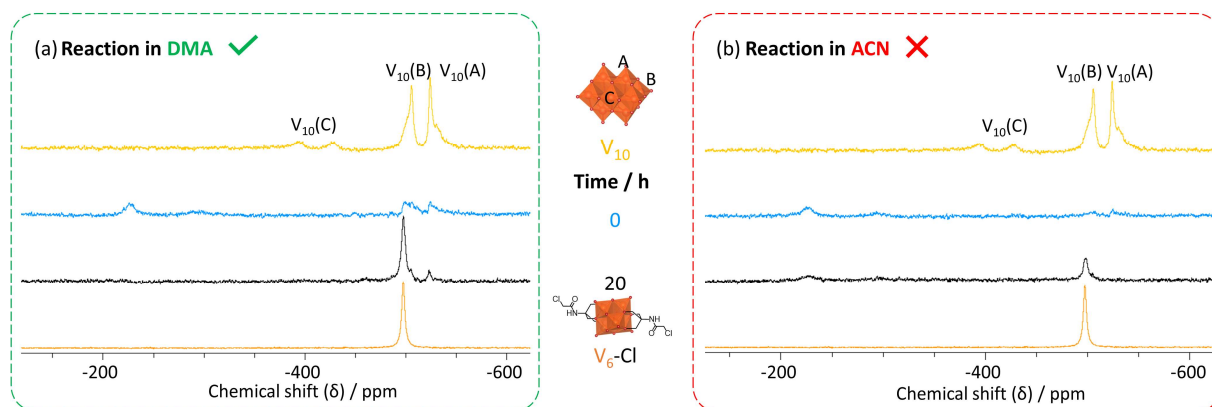


Figure S7 ^{51}V NMR spectrum of V_{10} alone as well as the spectra of aliquots of a mixture of V_{10} with Tris-Cl after heating at 80 °C for 0 and 20 h in (a) DMA or (b) ACN compared to the spectrum of pure $\text{V}_6\text{-Cl}$ (top to bottom). All spectra were acquired for solutions in ACN- d_3 .

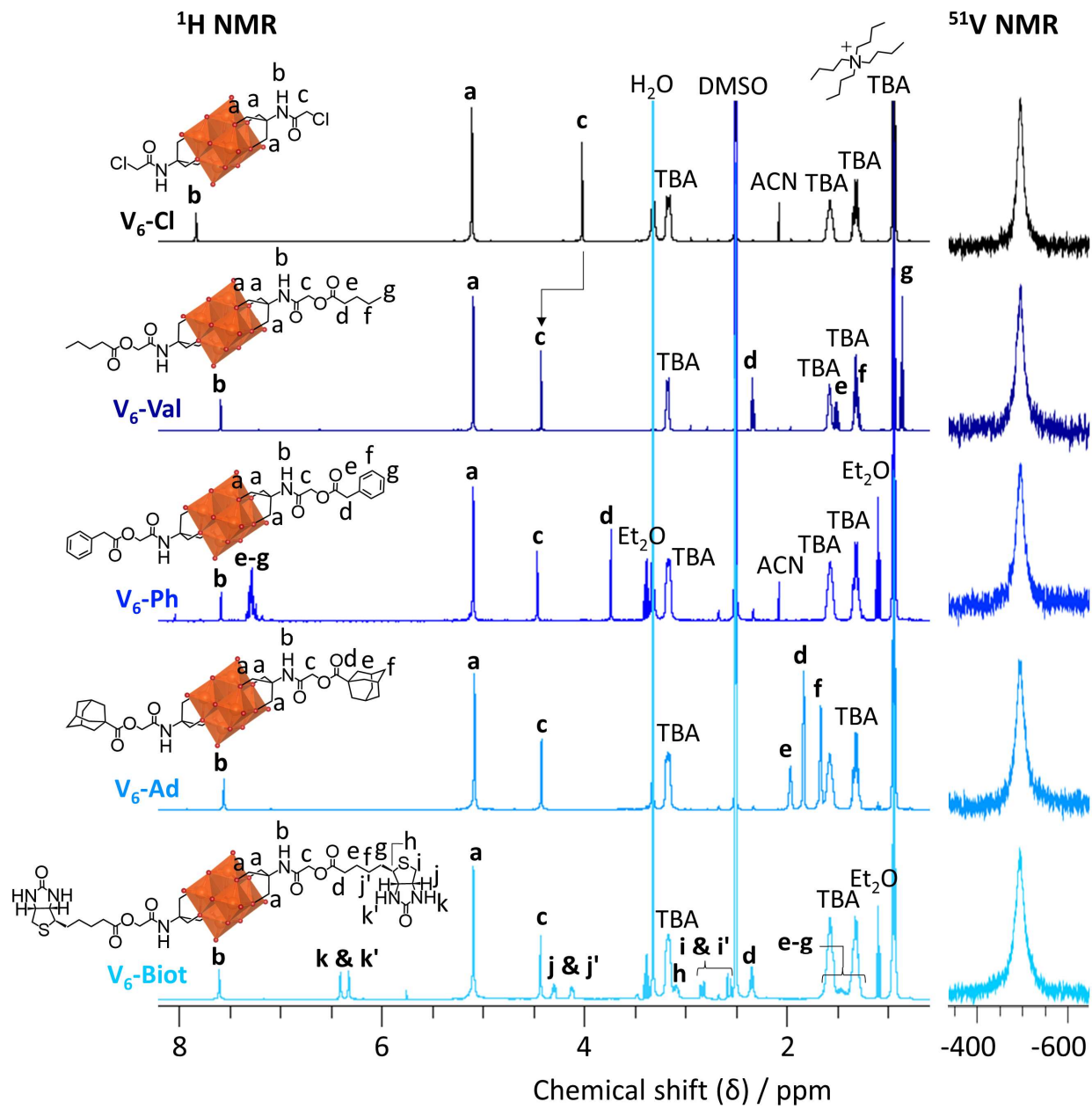


Figure S8 ^1H and ^{51}V NMR spectra of $\text{V}_6\text{-Cl}$, $\text{V}_6\text{-Val}$, $\text{V}_6\text{-Ph}$, $\text{V}_6\text{-Ad}$, and $\text{V}_6\text{-Biot}$ (top to bottom) in DMSO-d_6 .

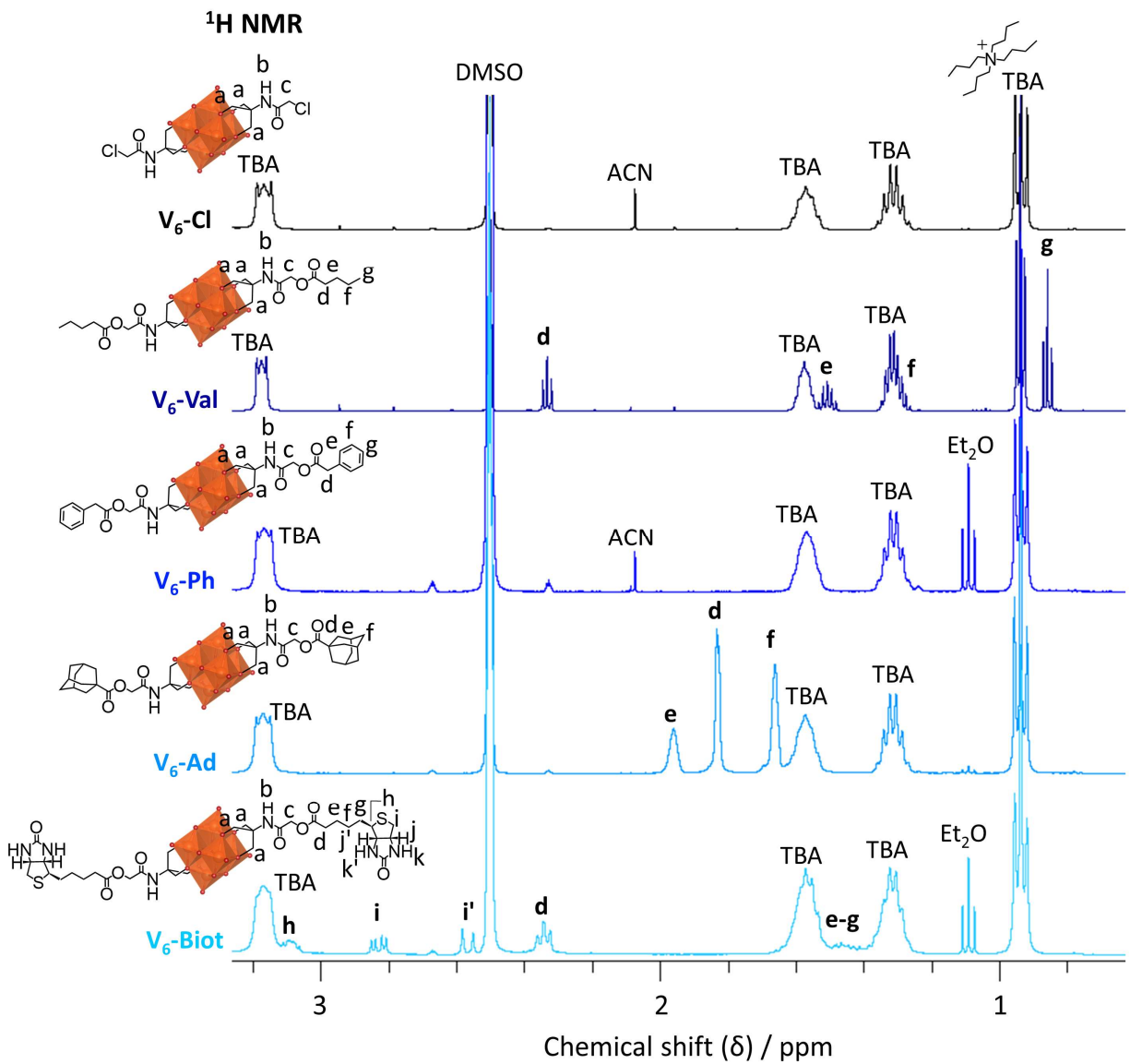


Figure S9 Close-up of ¹H NMR spectra of V₆-Cl, V₆-Val, V₆-Ph, V₆-Ad, and V₆-Biot (top to bottom) in DMSO-d₆.

UV-Vis-NIR Absorbance

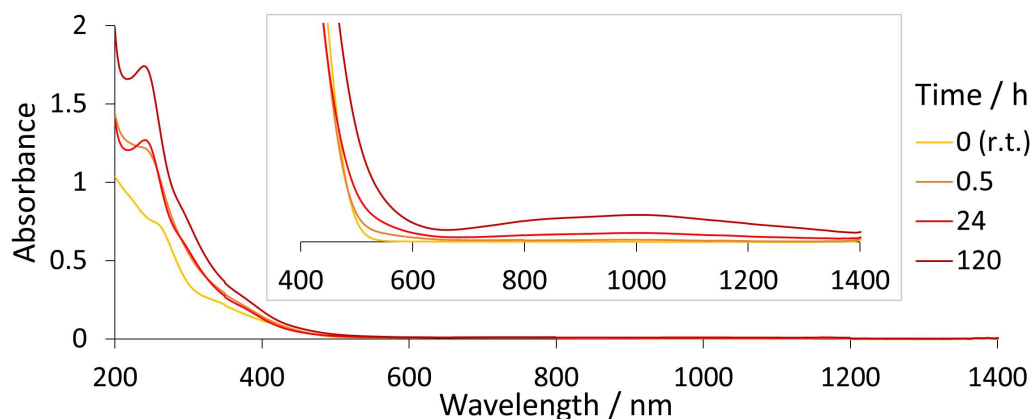


Figure S10 UV-Vis-NIR absorbance spectra of ACN solutions of V₁₀ after mixing at room temperature (r.t.) and after 0.5, 24, and 120 h at 80 °C. The broad IVCT peak observed for a more concentrated solution is shown in the insert.

Table S3 Maximum absorbance (A_{\max}) and wavelength (λ_{\max}) in the range 600-1400 nm of V₁₀ with Tris-NH₂ after mixing at room temperature and after 0.5, 24, and 120 h at 80 °C in ACN.

Time / h	A_{\max}	λ_{\max} / nm
0 (r.t.)	/	/
0.5	0.1589	718
24	0.2664	945
120	0.6531	887

Table S4 Maximum absorbance (A_{\max}) and wavelength (λ_{\max}) in the range 600-1400 nm of V₁₀ with Tris-Cl after mixing at room temperature and after 0.5, 24, and 120 h at 80 °C in ACN.

Time / h	A_{\max}	λ_{\max} / nm
0 (r.t.)	/	/
0.5	0.2512	940
24	0.4291	958
120	0.8179	976

IR Spectra

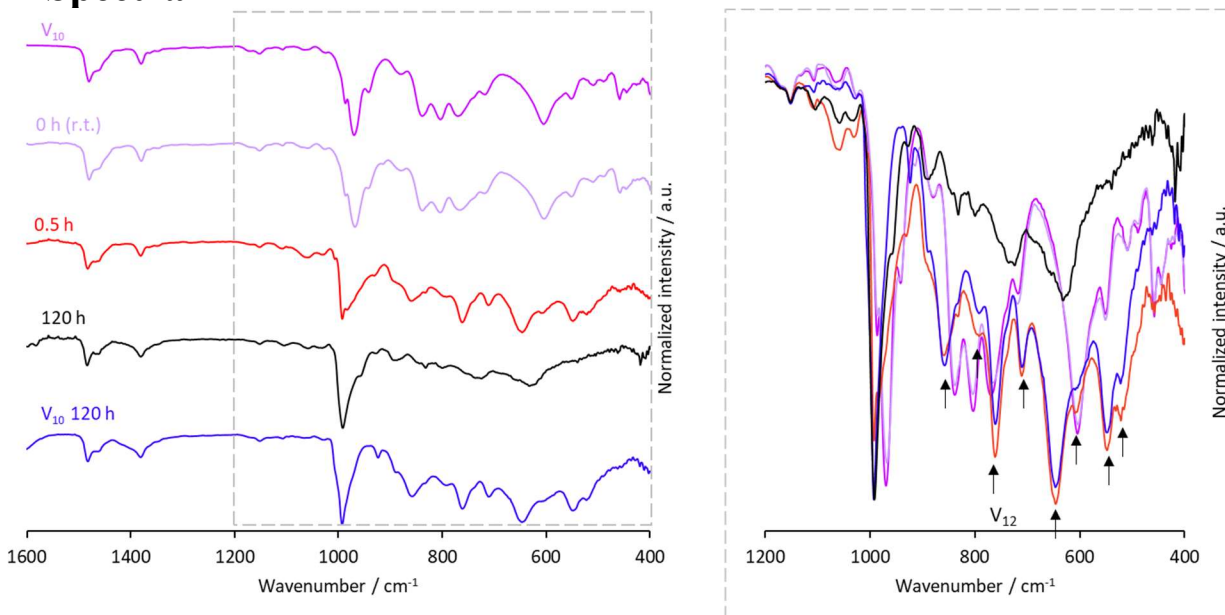


Figure S11 IR spectra of V_{10} alone at room temperature (top; purple) and after 120 h at 80 °C in $ACN-d_3$ (bottom; blue) as well as of V_{10} with $Tris-NH_2$ at room temperature (r.t.) and after 0.5 and 120 h at 80 °C in $ACN-d_3$ (light purple, red, and black). The peaks corresponding to $[V_{12}O_{32}]^{4-}$ (V_{12}) are indicated with arrows in the insert showing the overlaid spectra in the fingerprint region.

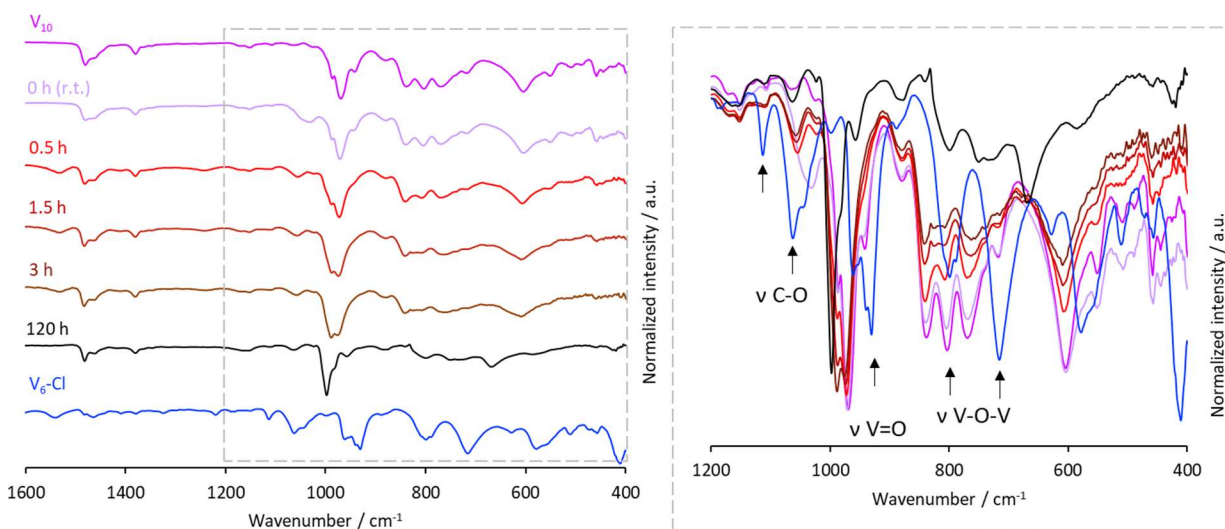


Figure S12 IR spectra of V_{10} alone at room temperature (top; purple) as well as of V_{10} with $Tris-Cl$ at room temperature (r.t.) and after 0.5, 1.5, 3 and 120 h at 80 °C in $ACN-d_3$ (light purple, red, dark red, brown, and black), which can be compared to the isolated pure V_6-Cl (bottom; blue). The peaks corresponding to V_6-Cl are indicated with arrows in the insert showing the overlaid spectra in the fingerprint region.

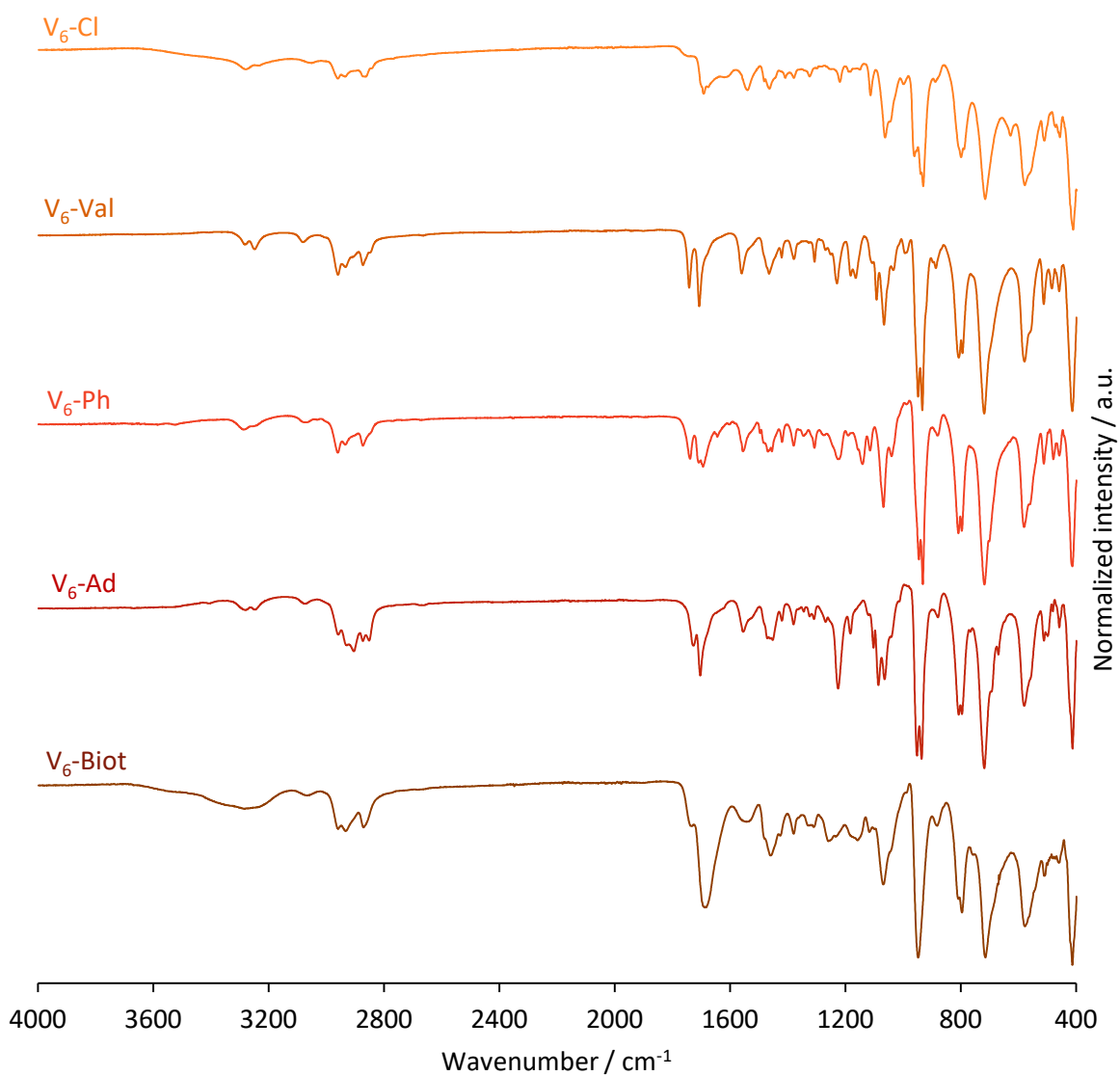


Figure S13 IR spectra of V₆-Cl, V₆-Val, V₆-Ph, V₆-Ad and V₆-Biot (top to bottom).

ESI-MS

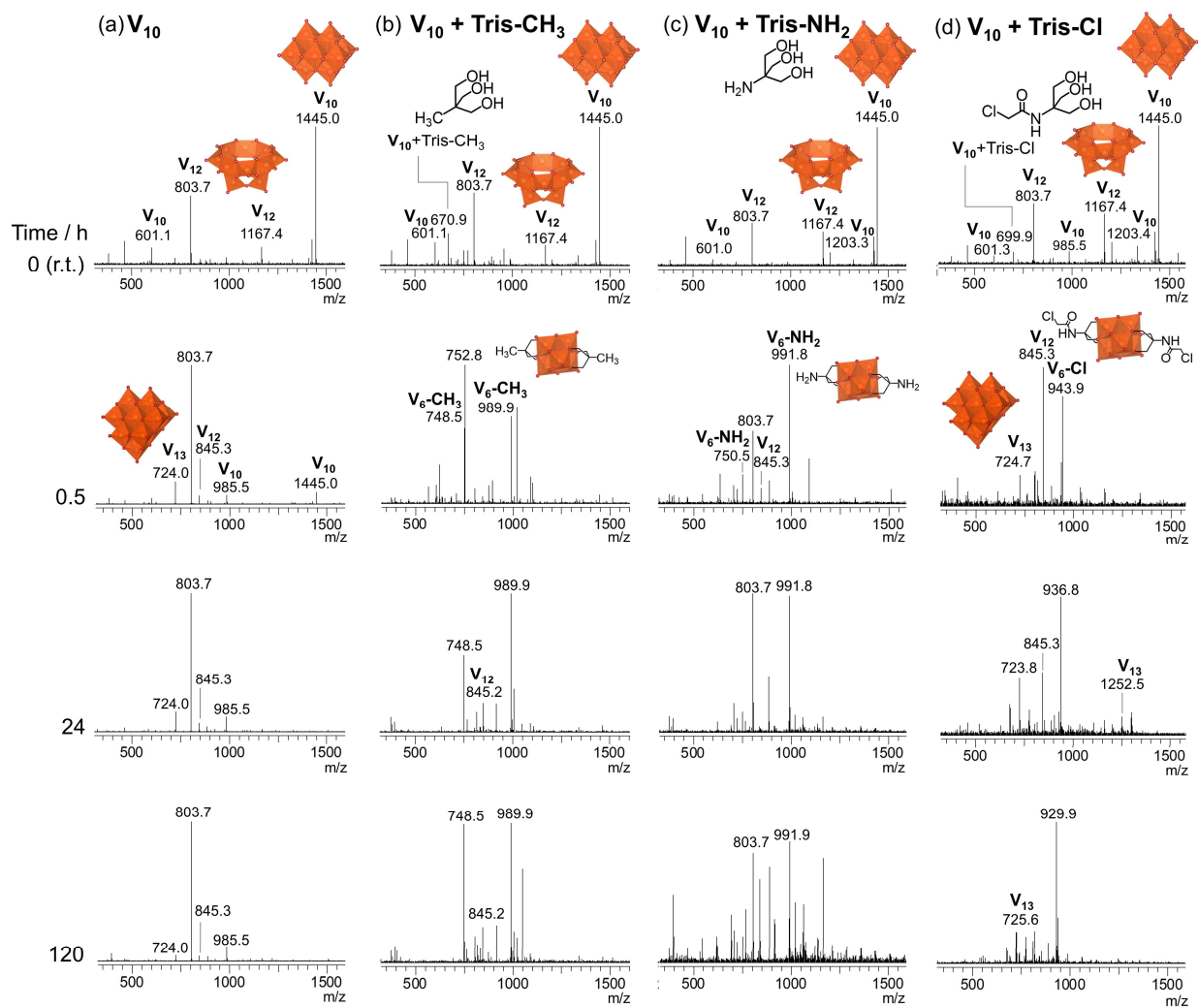


Figure S14 Negative mode ESI-MS of V_{10} in ACN (a) in the absence and in the presence of (b) Tris- CH_3 , (c) Tris- NH_2 or (d) Tris-Cl after mixing at room temperature (r.t.) and after 0.5, 24, and 120 h at 80 °C.

Table S5 Negative mode ESI-MS peak assignment for V₁₀ heated at 80 °C in ACN.
$$V_{10} = [H_3V_{10}O_{28}]^{3-}; V_{12} = [V_{12}O_{32}]^{4-};$$

$$V_{13} = [V_{13}O_{34}]^{3-}; TBA = [(C_4H_9)_4N]^+$$

Assignment	Calcd. m/z	Observed m/z
[V ₁₀ +TBA] ²⁻	601.5	601.1
[V ₁₃ +TBA] ²⁻	724.3	724.0
[V ₁₂ +2TBA] ²⁻	804.1	803.7
[V ₁₂ +2TBA+2ACN] ²⁻	845.2	845.3
[V ₁₀ +Na+H] ⁻	984.4	985.5
[V ₁₂ +3H+ACN] ⁻	1167.4	1167.4
[V ₁₀ +2TBA] ⁻	1445.3	1445.0

Table S6 Negative mode ESI-MS peak assignment for V₁₀ heated at 80 °C with Tris-CH₃ in ACN.
$$V_{10} = [H_3V_{10}O_{28}]^{3-}; V_{12} = [V_{12}O_{32}]^{4-};$$

$$V_6\text{-CH}_3 = [V_6O_{13}\{(OCH_2)_3CCH_3\}_2]^{2-}; TBA = [(C_4H_9)_4N]^+$$

Assignment	Calcd. m/z	Observed m/z
[V ₁₀ +TBA] ²⁻	601.5	601.1
[V ₁₀ +TBA+Tris-CH ₃ +H ₂ O] ²⁻	670.5	670.9
[V ₆ -CH ₃ +H] ⁻	748.9	748.5
[V ₁₂ +2TBA] ²⁻	804.1	803.7
[V ₁₂ +2TBA+2ACN] ²⁻	845.2	845.2
[V ₆ -CH ₃ +TBA] ⁻	990.4	989.9
[V ₁₂ +3H+ACN] ⁻	1167.4	1167.4
[V ₁₀ +2TBA] ⁻	1445.3	1445.0

Table S7 Negative mode ESI-MS peak assignment for V₁₀ heated at 80 °C with Tris-NH₂ in ACN.
$$V_{10} = [H_3V_{10}O_{28}]^{3-}; V_{12} = [V_{12}O_{32}]^{4-};$$

$$V_6\text{-NH}_2 = [V_6O_{13}\{(OCH_2)_3CNH_2\}_2]^{2-}; TBA = [(C_4H_9)_4N]^+$$

Assignment	Calcd. m/z	Observed m/z
[V ₁₀ +TBA] ²⁻	601.5	601.0
[V ₆ -NH ₂ +H] ⁻	750.9	750.5
[V ₁₂ +2TBA] ²⁻	804.1	803.7
[V ₁₂ +2TBA+2ACN] ²⁻	845.2	845.3
[V ₆ -NH ₂ +TBA] ⁻	992.3	991.8
[V ₁₀ +TBA+H] ⁻	1203.9	1203.3
[V ₁₀ +2TBA] ⁻	1445.3	1444.8

Table S8 Negative mode ESI-MS peak assignment for V₁₀ heated at 80 °C with Tris-Cl in ACN.

Assignment	Calcd. m/z	Observed m/z
[V ₁₀ +TBA] ²⁻	601.5	601.3
[V ₁₀ +TBA+Tris-Cl] ²⁻	700.3	699.9
[V ₁₃ +TBA] ²⁻	724.3	723.8 / 724.7
[V ₁₂ +2TBA] ²⁻	804.1	803.7
[V ₁₂ +2TBA+2ACN] ²⁻	845.2	845.3
[V ₆ -Cl+H+ACN] ⁻	945.7	943.9
[V ₁₀ +Na+H] ⁻	984.4	985.5
[V ₁₂ +3H+ACN] ⁻	1167.4	1167.4
[V ₁₀ +TBA+H] ⁻	1203.9	1203.4
[V ₁₃ +2Na] ⁻	1252.2	1252.5
[V ₁₀ +2TBA] ⁻	1445.3	1445.0

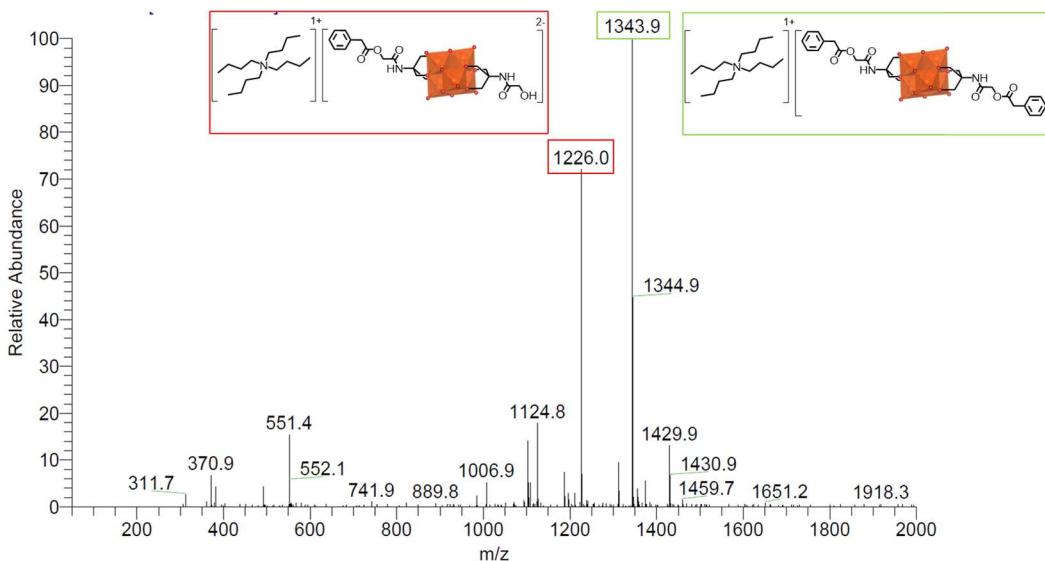


Figure S15 Negative mode ESI-MS of the reaction mixture for the synthesis of V₆-Ph with TBA-OH after 6 h. Peak corresponding to the target compound in green and the target compound hydrolysed on one side in red.

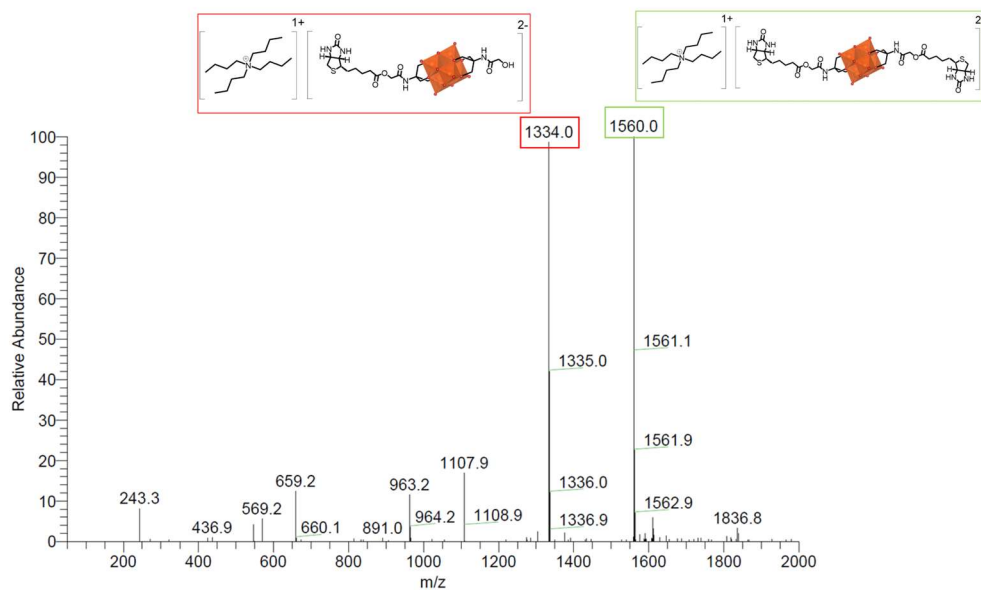


Figure S16 Negative mode ESI-MS of the reaction mixture for the synthesis of V₆-Biot with TBA-OH after 24 h. Peaks corresponding to the target compound in green and the target compound hydrolysed on one side in red.

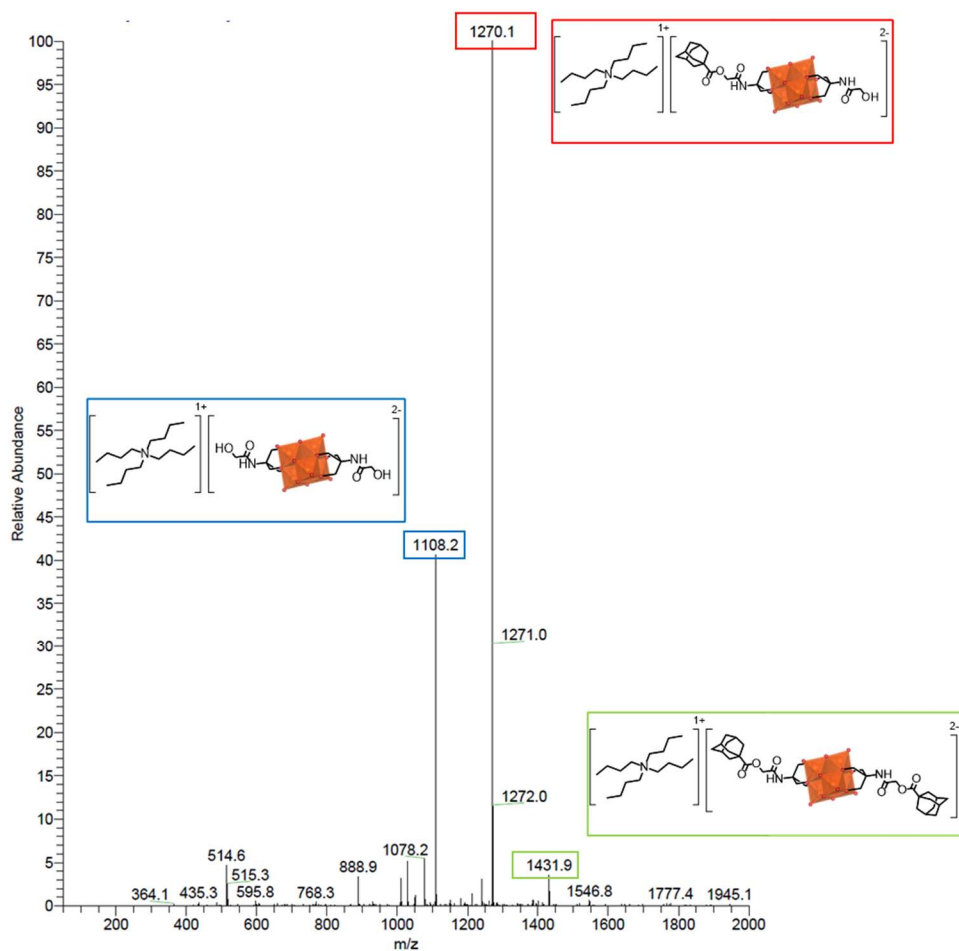


Figure S17 Negative mode ESI-MS of the reaction mixture for the synthesis of V₆-Ad with TBA-OH after 48 h. Peaks corresponding to the target compound in green, the target compound hydrolysed on one side in red, and the target compound hydrolysed on both sides in blue.

CV

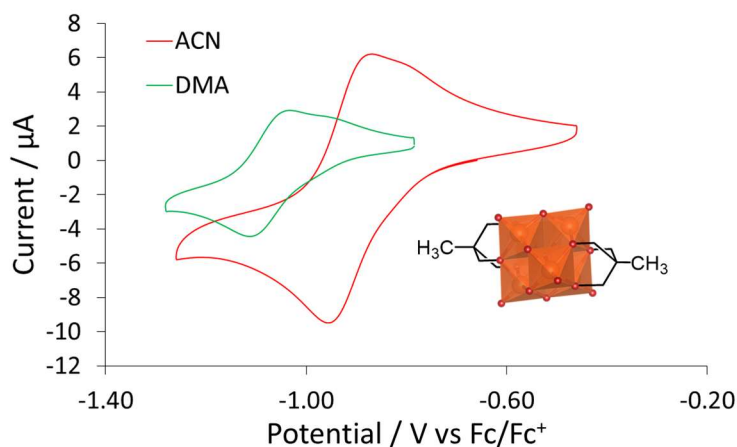


Figure S18 CV of 0.5 mM V_6-CH_3 in ACN vs in DMA with 0.1 M TBA- PF_6 as the electrolyte (100 mVs^{-1}).

References

1. Rigaku Oxford Diffraction, 2019, CrysAlisPro Software system, Rigaku Corporation, Oxford, UK.
2. O. V. Dolomanov, L. J. Bourhis, R. J. Gildea, J. A. K. Howard and H. Puschmann, *Journal of Applied Crystallography*, 2009, **42**, 339–341.
3. G. M. Sheldrick, *Acta Crystallographica Section A Foundations and Advances*, 2015, **71**, 3–8.
4. G. M. Sheldrick, *Acta Crystallographica Section C Structural Chemistry*, 2015, **71**, 3–8.
5. W. G. Klemperer, in *Inorganic Syntheses*, ed. A. P. Ginsberg, John Wiley & Sons, Inc., Hoboken, NJ, USA, 1990, vol. 27, pp. 74–85.
6. S. Vanhaecht, T. Quanten and T. N. Parac-Vogt, *Inorganic Chemistry*, 2017, **56**, 3095–3101.
7. D. Rehder, T. Polenova and M. Bühl, in *Annual Reports on NMR Spectroscopy*, 2007, vol. 62, pp. 49–114.